

Dynamic upwelling beneath the Salton Trough imaged with teleseismic attenuation tomography

Joseph S. Byrnes^{1*} and Maximiliano Bezada¹

¹Department of Earth Sciences, University of Minnesota, 116 Church Street SE

Minneapolis, MN 55455 USA

To whom correspondence should be addressed; Email jsbyrnes@umn.edu

Contents of this file

Text S1 to S2
Figures S1 to S3

Introduction

This supplement provides two alternative inversions of the data and an alternative plot of the preferred result. As the preferred model is discussed in detail in the main text, no Earth structure will be inferred here. Methodological details are also provided in the main text.

Text S1. Inversion of the data with damped least squares.

In the main text, we invert synthetic datasets with both the damped-least squares and Bayesian approaches. The Bayesian approach better recovered the shape and amplitude of anomalies. While we do not interpret the inversion of the data from damped least squares, we show the results here for completeness. The smoothing and damping parameters are chosen based on the curvature of the natural log of the misfit against regularization parameters (Figure S1a). When inverting without enforcing a discontinuity, the primary anomaly is a vertical ellipse centered at the surface with an amplitude that decreases with increasing depth. In contrast, when a discontinuity is enforced, attenuation occurs both above and below the discontinuity, with a marginally larger anomaly in the asthenosphere. Overall amplitudes are small relative to the results from the preferred approach (Figure 9a of the main text).

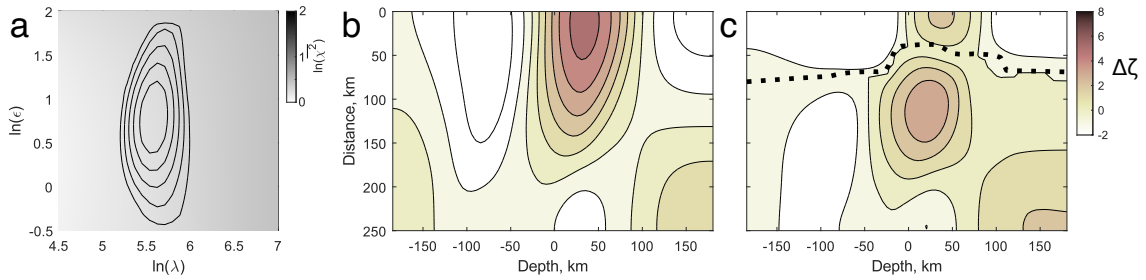


Figure S1. Inversion of the data with damped least squares. cf. Fig. 6 of the main text. A) Misfit is shown by grays and the curvature of the misfit surface is shown by black contours. B) Colors contour amplitude of $\Delta\zeta$ anomalies. C) Same as B), except for the dashed line which indicates the discontinuity enforced on this inversion.

Text S2. Inversions of the data with Bayesian approach.

In the main text, we show an inversion of the data with the Bayesian approach with a discontinuity enforced. In Figure S2a, we show the same inversion as in Figure 9a, but with the limits of the plot extend to regions of model space with poor ray-path coverage. This is the same inversion as in Figure 9a; only the dimensions of the figure are different. The largest anomaly outside of the space shown in Figure 9a is a negative anomaly that peaks at $\Delta\zeta = -10$ at a depth of ~ 225 km. This anomaly is not required (Figure S3a, orange line) as the PDF is bimodal, with a secondary peak allowing a $\Delta\zeta \sim 0$ at the same location. No other prominent structures occur outside of the region plotted in Figure 9a.

In Figure S2b, we show an inversion without the discontinuity enforced. In this case, the attenuation extends across where the discontinuity would have been placed (cf. Figure S1b). As discussed in the main text, this is physically implausible as a layer with high V_s occurs above the discontinuity that will impose some change in the Qp structure.

Moreover, while there is no prominent negative anomaly at ~ 225 km depth similar to that in Figure S2a (Figure S3a), there is a negative anomaly at ~ 120 km depth on the eastern (positive direction on the x-axis) side of the study area. This anomaly is again not required and the PDFs at this point is bimodal in inversions both including and excluding the discontinuity (Figure 3b). We also note that the PDFs are markedly tighter when the discontinuity is included. The preferred inversion is therefore more physically plausible, returns more certain results, and does not feature an implausible negative anomaly adjacent to the attenuation maximum discussed in the main text.

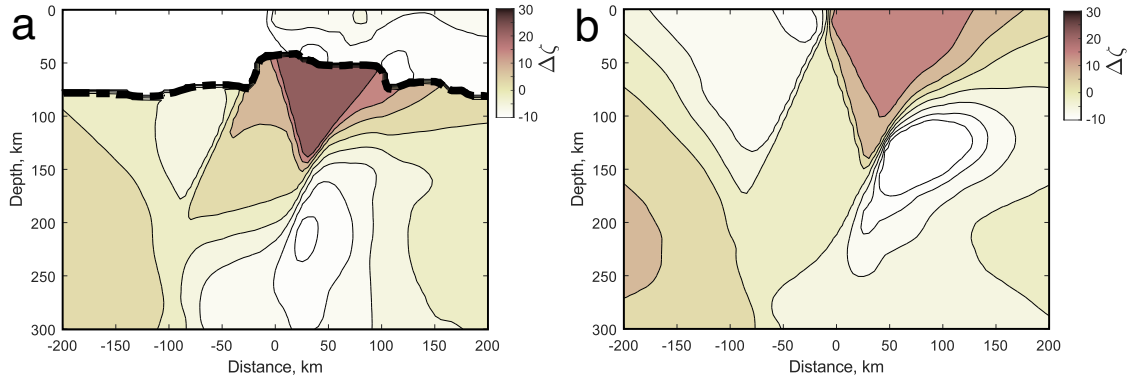


Figure S2. Inversion of the data with the Bayesian approach. cf. Fig. 9 of the main text. A) Colors contour the median of the ensemble from the Bayesian inversion; see main text for the contouring interval. Black dashed line marks the discontinuity. B) Colors contour the median of the ensemble from the Bayesian inversion with no discontinuity enforced.

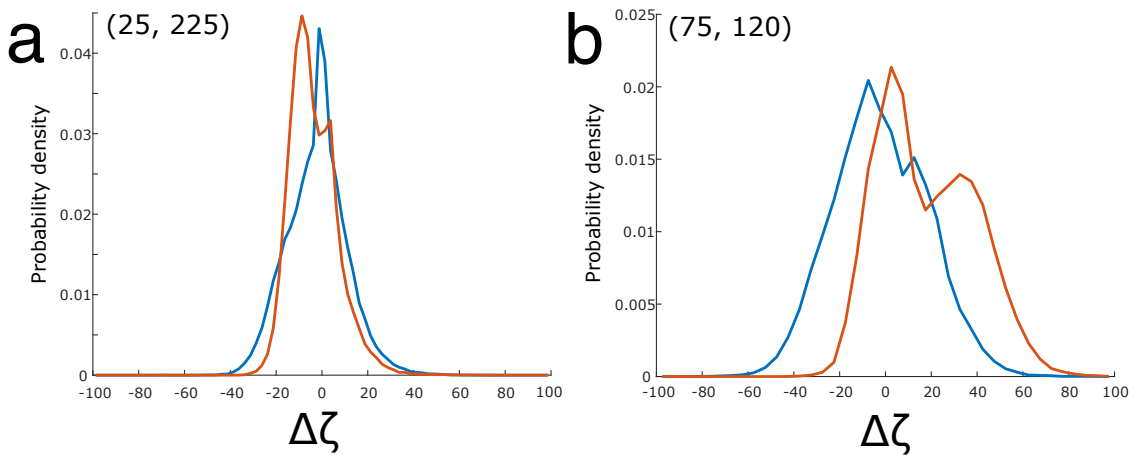


Figure S3. Probability density functions for $\Delta\zeta$ at different points in the inversions. Orange and blue refer to the models in Figure S2a and S2b, respectively. Text in the top left gives the locations at which the PDFs are taken along the x and y axes, respectively.